Acta Cryst. (1975). A31, 794

High-Resolution Electron Microscopy and Diffraction Studies of Fibrous Amphiboles

BY J. L. HUTCHISON

Inorganic Chemistry Laboratory, South Parks Road, Oxford, England

AND M. C. IRUSTETA AND E. J. W. WHITTAKER

Department of Geology and Mineralogy, Parks Road, Oxford, England

(*Received* 14 *April* 1975; *accepted* 21 *May* 1975)

Fibrous specimens of tremolite, amosite, crocidolite and anthophyllite have been studied by electron diffraction and high-resolution microscopy. Amosite (and to a lesser extent crocidolite) are shown to be subject to frequent twinning on (100) leading to stacking disorder, and an explanation is provided of previously supposed anomalies in their diffraction patterns [Chisholm (1973), *J. Mater. Sci.* **8**, 475–483]. Tremolite is sensibly free from these defects and this is explained in terms of crystal chemistry. The presence of Wadsley defects of the type suggested by Chisholm has been confirmed in tremolite, amosite and anthophyllite, and these defects have been shown to correspond to intercalation of lamellae of triple-chain structure parallel to (010). In anthophyllite these lamellae are observed to segregate into domains.

1. Introduction

The silicate chain structure of the amphiboles, shown by Warren (1930) to account for the cleavage properties of these minerals, has commonly been assumed also to account for their occurrence in asbestiform varieties, notwithstanding that single crystals of the amphibole certainly do not cleave into fine fibres. In spite of the large number of X-ray structure refinements of amphiboles in recent years, specific studies of fibrous varieties have been few. Rabbitt (1948) showed by X-ray diffraction that amosite, previously classified as orthorhombic, was in fact monoclinic and a fibrous form of grunerite. It approximates in composition to $Fe_6MgSi_8O_{22}(OH)_2$. Whittaker (1949) reported a structure refinement of an unusually thick fibre of a crocidolite, which was really a twinned single crystal of magnesio-riebeckite composition near $Na_2Mg_3Fe_2^{3+}Si_8O_{22}$. Whittaker (1950) also reported on the existence of disorder in fibrous anthophyllite and in amosite, and suggested that, in the latter at least, this was associated with some kind of longitudinal displacements of the chains. A preliminary X-ray study of amosite was reported by Garrod & Rann (1952) and the structure of grunerite was refined by Finger (1969).

Electron micrographs of amphiboles, and selected-area diffraction patterns, have been presented by Zvyagin & Gorshkov (1969), together with the methods for indexing some of the patterns that can be obtained. These were, however, confined to sections of the reciprocal lattice containing **y***. Some very fine high-resolution electron micrographs of kaersutite have been presented by Buseck & Iijima (1974) showing structural faulting in projections on the *xy* and *yz* planes.

Chisholm (1973) has studied both amosite and crocidolite by electron microscopy and selected-area diffraction. He has presented diffraction patterns which he interpreted as y^*z^* sections of the reciprocal lattice, and has pointed out some anomalous features in these patterns, namely:

(i) $0kl$ reflexions with k (and $k+l$) odd, violating the space-group absences for $C2/m$ (or its alternative setting $I2/m$), which cannot arise through double reflexion;

(ii) little change in the pattern for a variety of tilts of the specimen about the y^* axis;

(iii) weak continuous streaks of intensity along **y***. He suggests (iii) to be due to the presence of Wadsley defects in the structure, corresponding to occasional layers parallel to (010) containing either pyroxene single chains instead of amphibole double chains, or alternatively (or perhaps in addition) triple or multiple chains intermediate in composition between amphibole and talc. The correctness of this suggestion is strikingly demonstrated in the present work. Chisholm's suggestion to account for (i) and (ii) is that the intensity distribution in reciprocal space is continuous along rods parallel to **x*** through the points corresponding to the $0kl$ nodes of the reciprocal lattice; that is, the expected hkl reflexions are broadened in the **x*** direction to the extent that they have a substantial intensity over a range up to $\pm a^*$ from their expected maxima. He suggested that this phenomenon could be due to frequent twinning on (100). The existence of a certain amount of twinning of this kind is confirmed, and will be illustrated further in the present paper. However, the details of Chisholm's assumptions are incompatible with the X-ray diffraction patterns of amosite and crocidolite and with a fuller investigation of the

electron diffraction patterns themselves, and are shown to be unnecessary in explaining the phenomena that he described.

2. Experimental

Small fragments were removed from the various specimens and embrittled in liquid nitrogen before being crushed in a percussion mortar, also previously cooled in liquid nitrogen. The material thus prepared was suspended in chloroform, dispersed by ultrasonic treatment and mounted on carbon-coated Cu grids.

The specimens were examined in a Siemens Elmiskop 102 with 125 kV accelerating voltage. In order to obtain satisfactory results it was found to be essential to use an accurately calibrated $\pm 45°$ double-tilt stage incorporating a z-axis adjustment. Using this device, it was possible to record series of electron diffraction patterns from single fibres, over very large variations in tilt angle (up to 90°) while maintaining the lens settings constant. In this way camera length errors due to tilt variations were completely eliminated and a series of rational sections of the reciprocal lattice could be unambiguously indexed.

Lattice images were recorded at magnifications of between 3×10^5 and $7{\cdot}5\times10^5$. A 50 μm objective aperture allowed beams down to 3 Å (real space) to contribute to the image.

The specimens used were: amosite from Penge, Transvaal; crocidolite from Golling, Salzburg (Figs. 2 and 9) and also from Heuningvlei, South Africa; tremolite from Turkey; and anthopyllite from Paakila, Finland.

3. Electron diffraction patterns of amphibole

Some published electron diffraction patterns of amphibole (*e.g.* Clark & Ruud, 1974) appear to have been produced from thick crystals (> 500 Å). Such patterns are frequently very complex, with many spots, and an example is shown in Fig. 1. The complexity may be due in part to the crystals being composite and containing portions in a number of different orientations around the z axis (this is likely in the case of fibrous varieties), and in part to multiple scattering. We have not found it profitable to try to interpret such patterns. In order to obtain good patterns the specimens should be transparent in the electron micrograph. However, even then there are a number of problems involved in recognizing the orientation of amphibole crystallites, and a well-calibrated double-axis tilting stage is essential.

Because of the prismatic (110) cleavage of single crystals and the extension of fibres parallel to [001], amphibole specimens are almost always elongated parallel to [001], and lie on the grid with this axis near to horizontal. The difficulties arise partly from the prevalence of twinning on (100), and partly from certain approximate equalities between various parameters of the clino-amphibole lattice. Some of these have been discussed by Whittaker & Zussman (1961), and indexing is here kept entirely in terms of the setting $C2/m$ for the space group of the clino-amphiboles. From the point of view of electron diffraction, the important coincidences for clino-amphiboles are:

$$d_{001}\simeq d_{\bar{1}01}$$
$$3c^*\cos\beta\simeq a^* \text{ for grunerite}$$
$$2c^*\cos\beta\simeq a^* \text{ for tremolite}$$
$$a^*\simeq 2b^*\,.$$

For ortho-amphiboles there is the very confusing coincidence

$$a^*\simeq b^*\,.$$

The simplest diffraction patterns to interpret are those obtained when the crystal lies with its (010) plane perpendicular to the electron beam. Two examples are shown in Fig. 2(*a*) and (*b*) which were obtained from amosite and crocidolite respectively. They show the presence of two orientations of the x^*z^* section of the reciprocal lattice present together, an effect that is compatible with twinning by reflection on (100). The $h0l$ reflexions occur only for h even, as expected from the space group $C2/m$. The two patterns differ principally in the degree to which the reflexions are streaked along the layer lines, which is much greater in the case of amosite. The streaking is most intense on the second layer line, and weakest on the third, although here the spots are also weak. Streaking is present on the zero layer line of Fig. 2(*a*), but this is a variable feature, and its intensity is low relative to the very strong spots; this streaking cannot be attributed directly to twinning, since a crystal twinned on (100) would diffract as a single coherent domain for the $h00$ reflexions, but it may be due to double reflexion from $h0l$ and $h0\bar{l}$. The lack of resolution of the twin reflexions on the third layer line of amosite is due to the value of β which causes them almost to coincide. The streaking, even for amosite, is clearly not so intense as to prevent substantial differences occurring between different sections of reciprocal space containing $\mathbf{y}^*$, as was postulated by Chisholm (1973).

It has proved impossible to find tremolite fibres either lying on (010), or sufficiently near to that orientation to permit (010) to be brought perpendicular to the beam by tilting. However, the diffraction patterns obtained with the beam perpendicular to (100) discussed below show that similar twinning does not occur in this material. If the specimens giving rise to the patterns of Fig. 2 are tilted through small angles then typical off-centre Laue zones are produced in the usual way.

If a clino-amphibole crystal lies with its (100) plane perpendicular to the beam (and therefore $\mathbf{x}^*$ parallel to the beam) no rational plane of the reciprocal lattice will be horizontal and only the row of $0k0$ reciprocal-lattice points will lie on the sphere of reflexion (treated as approximating to a plane). However, the angle between $\mathbf{x}^*$ and $[\bar{1}02]^*$ is very near to 90°, the calculated

value for tremolite being 89° 5′. Thus the rows of reciprocal-lattice points $\bar{1}k2$, $\bar{2}k4$ *etc.* will lie very close to the sphere of reflexion, while all other rows will be a distance of approximately $a^*/2$ from it, as shown in Fig. 3. Strictly, a slightly off-centre Laue zone will be obtained if the beam is exactly perpendicular to (100), but the nearest position with centred Laue zones will correspond to the above situation. An electron diffraction pattern of tremolite fibre in this orientation is shown in Fig. 4(*a*). The layer-line spacing in the central Laue zone is close to $2c^*$, and k is odd or even according as the layer line is odd or even, in accordance with the requirement that $h+k$ be even. If the crystal is tilted in the correct direction about its y axis by about 16°, the y^*z^* section is obtained [Fig. 4(*b*)]. Tilting in the other direction leads to a situation where successive rows are $\bar{1}kl$, $\bar{2}k2$, *etc.* [Fig. 4(*c*)]. Figs. 4(*b*) and 4(*c*) are superficially similar because of the approximate equality of d_{001} and $d_{\bar{1}01}$, but on Fig. 4(*b*) k is even throughout because $h=0$, whereas on Fig. 4(*c*) k is odd or even according as the layer line is odd or even. At the other orientations, intermediate between those illustrated, off-centre Laue zones develop in the usual way, and there is no evidence of material in a twinned orientation.

With a twinned crystal two orientations of the reciprocal lattice are present, as shown in Fig. 5, and the combination is symmetrical about the x^*y^* plane. For this reason no asymmetry of Laue zones will be visible when the beam is exactly perpendicular to (100). Because of the thinness of the twin lamellae, there is streaking of the reciprocal-lattice points parallel to $\mathbf{x}^*$, and this will reduce the visibility of any Laue zones that develop when the crystal is tilted,† but in addition to this effect there will be compensatory effects along $\pm\mathbf{z}^*$ when the tilt is about $\mathbf{y}^*$ as the points belonging to the two reciprocal lattices come into the reflecting position on opposite sides of the origin. An unexpected insensitivity of the pattern to tilt about $\mathbf{y}^*$ is therefore developed, as indicated by Chisholm (1973), though by no means entirely because of the reason that he adduced. A diffraction pattern of amosite in this orientation is shown in Fig. 6(*a*). Because for amosite it is the angle between $\mathbf{x}^*$ and [103]* that approximates to 90° (actually 88·7°) the layer lines observed are of the type $\bar{1}k3$, $\bar{2}k6$ *etc.* as indicated in Fig. 5. Weak intermediate rows are observed with $l=1$ and $l=2$ where the sphere of reflexion intersects the streaking parallel to $\mathbf{x}^*$ that was observed in Fig. 2(*b*).

When the fibre is tilted about the y axis by 12° to give the y^*z^* section of one of the reciprocal lattices [Fig. 6(*b*)], the diffraction pattern is rather surprising, in that all the $0kl$ reflexions appear. The centred lattice might be expected to give rise to reflexions only with k even, but the reflexions with k odd, although weaker, are far from negligible. On the first and second layer lines this may be partly explained by the presence of odd-k reciprocal-lattice points of the second lattice at distances the order of $a^*/3$ from the Ewald sphere. However, this does not explain the appearance of reflexions with k odd on the zero and third layer lines. These may be explained by double (or multiple) reflexions in which one reflexion takes place in one of the twin lamellae and another takes place in an oppositely oriented lamella. For example the combination of the vectors $0kl$ (k even) of one lattice with $1\bar{k}'l$ ($\bar{k}'$ odd) of the other (which is $a^*/3$ from the Ewald sphere) will give a double reflexion simulating $0, k+k', 2$ of the first lattice. Such inter-lamellar double reflexions contribute to all the layer lines. Because of the twinning an equal tilt from the position of Fig. 6(*a*) but in the opposite direction from Fig. 6(*b*) leads to the y^*z^* section of the other twin, and therefore a similar pattern [Fig. 6(*c*)]. A further tilt leads to a position [Fig. 6(*d*)] with layer lines containing reflexions of the type $\bar{h}kh$, which is distinguished from the previous two patterns by the fact that the strong reflexions have k odd on odd layer lines in accordance with the space group.

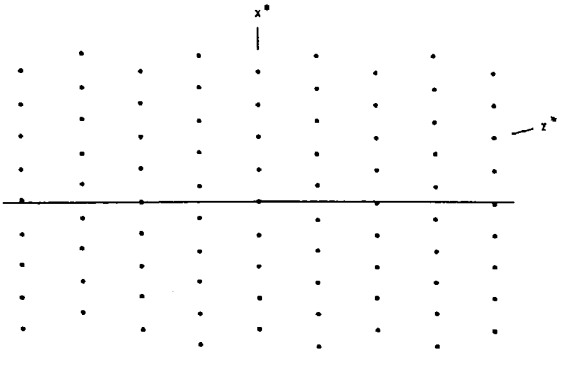

Fig. 3. Projection of the reciprocal lattice of tremolite down $\mathbf{y}^*$, with the electron beam parallel to $\mathbf{x}^*$.

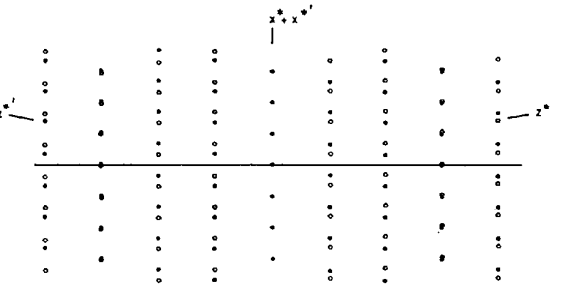

Fig. 5. Projection down $\mathbf{y}^*$ of the combined reciprocal lattices of an amosite twin. When the twin lies with [100] perpendicular to the beam, the position of the sphere of reflexion (approximated by a plane) is as shown. The filled and empty circles indicate the positions for the twin-related rows of reciprocal-lattice nodes parallel to $\mathbf{y}^*$. The positive direction of $\mathbf{y}^*$ is above the paper and that of $\mathbf{y}^{*\prime}$ below the paper.

† The magnitude of the effect will in fact be greater than would be expected on the basis of the streaking parallel to $\mathbf{x}^*$ visible in Fig. 2, because the diffuseness of the spots will be enhanced when $\mathbf{x}^*$ is approximately parallel to the beam (Pinsker, 1953).

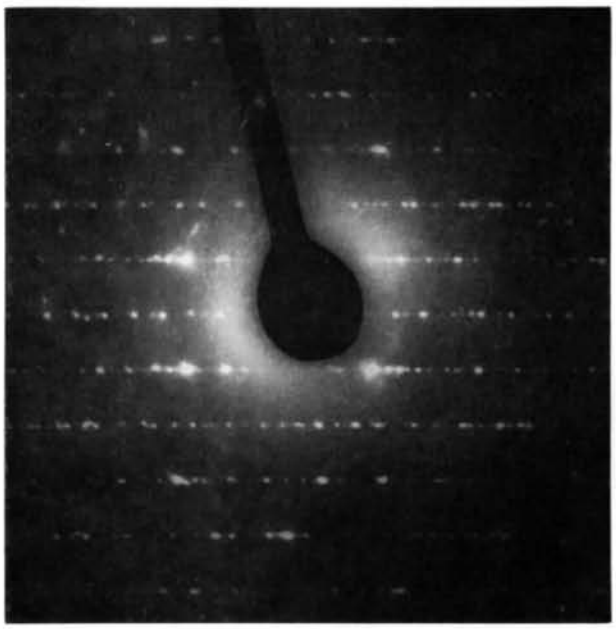

Fig. 1. Complex electron diffraction pattern given by a thick fibre of amosite.

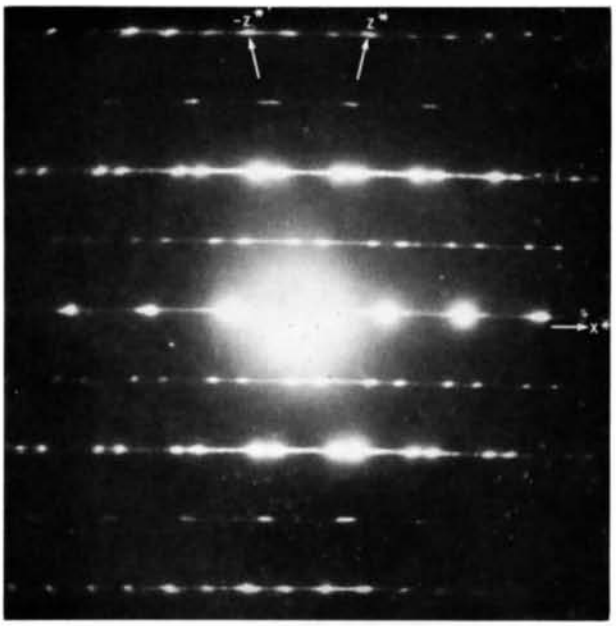

(*a*)

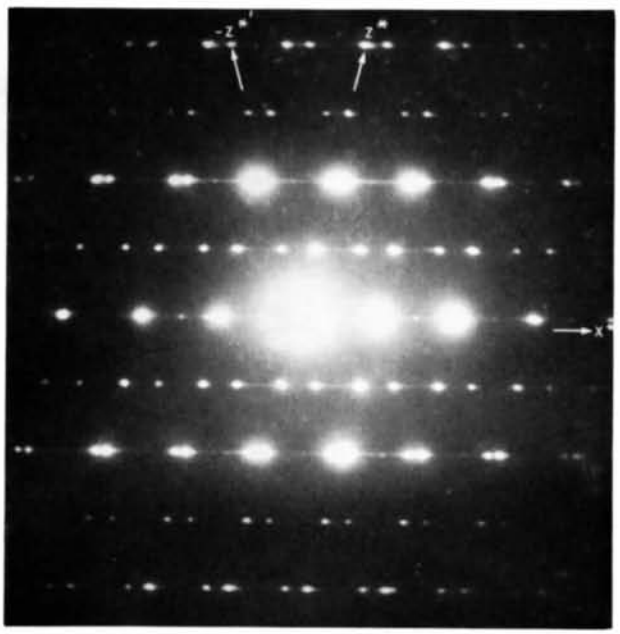

(*b*)

Fig. 2. Electron diffraction pattern with the beam parallel to [010], and containing the *h*0*l* reflexions. (*a*) amosite, (*b*) crocidolite. Both patterns show twinning on (100).

[*To face p.* 796

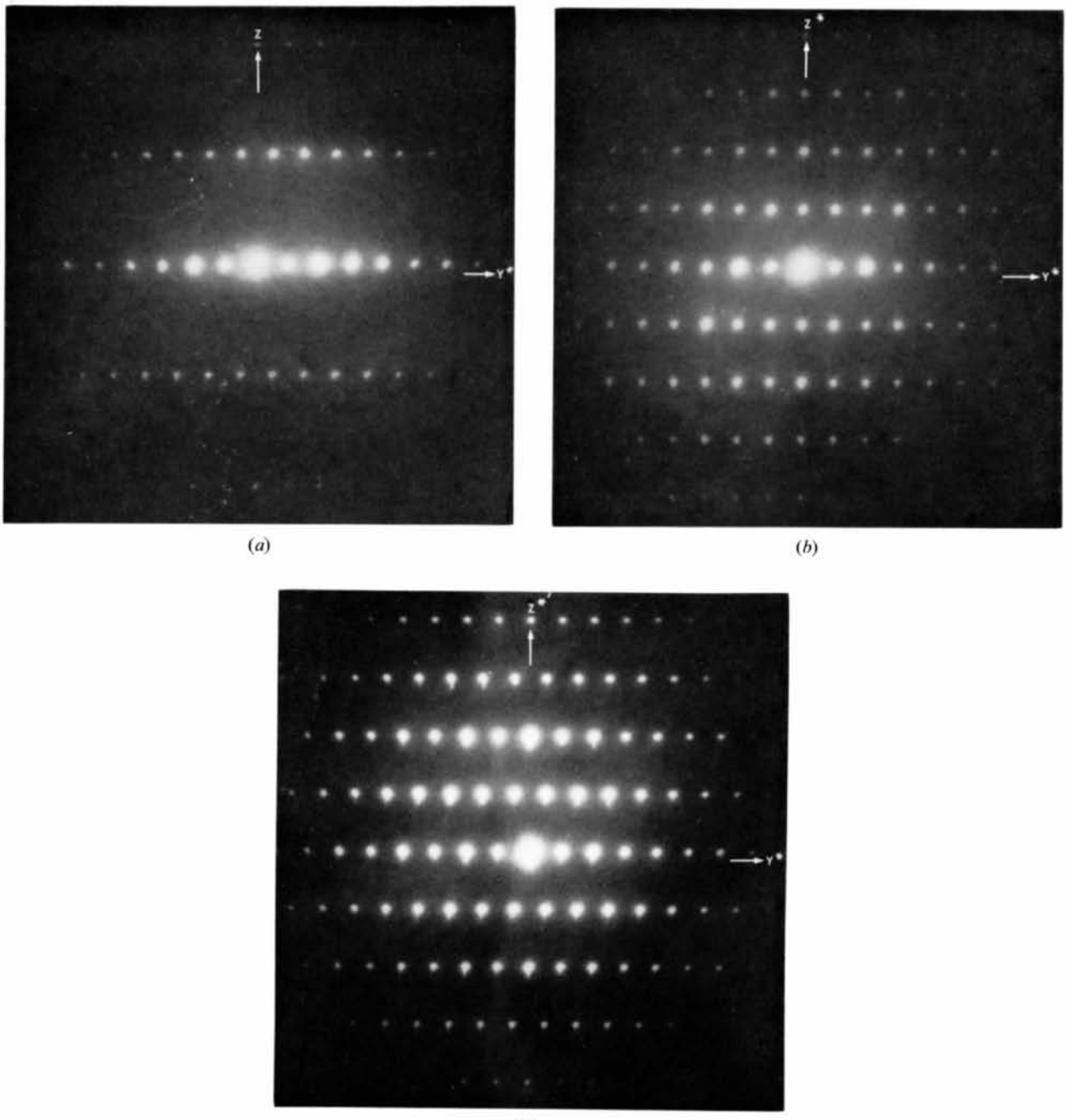

(*a*) (*b*)

(*c*)

Fig. 4. Electron diffraction patterns of tremolite: (*a*) beam (approximately) perpendicular to (100), giving reflexions of type $\bar{h},k,2h$; (*b*) specimen tilted by 16° about the *y* axis to give the beam parallel to **x**, and reflexions of type $0kl$; (*c*) specimen as (*a*) but tilted in the opposite direction from (*b*) to give reflexions of type $\bar{h}kh$.

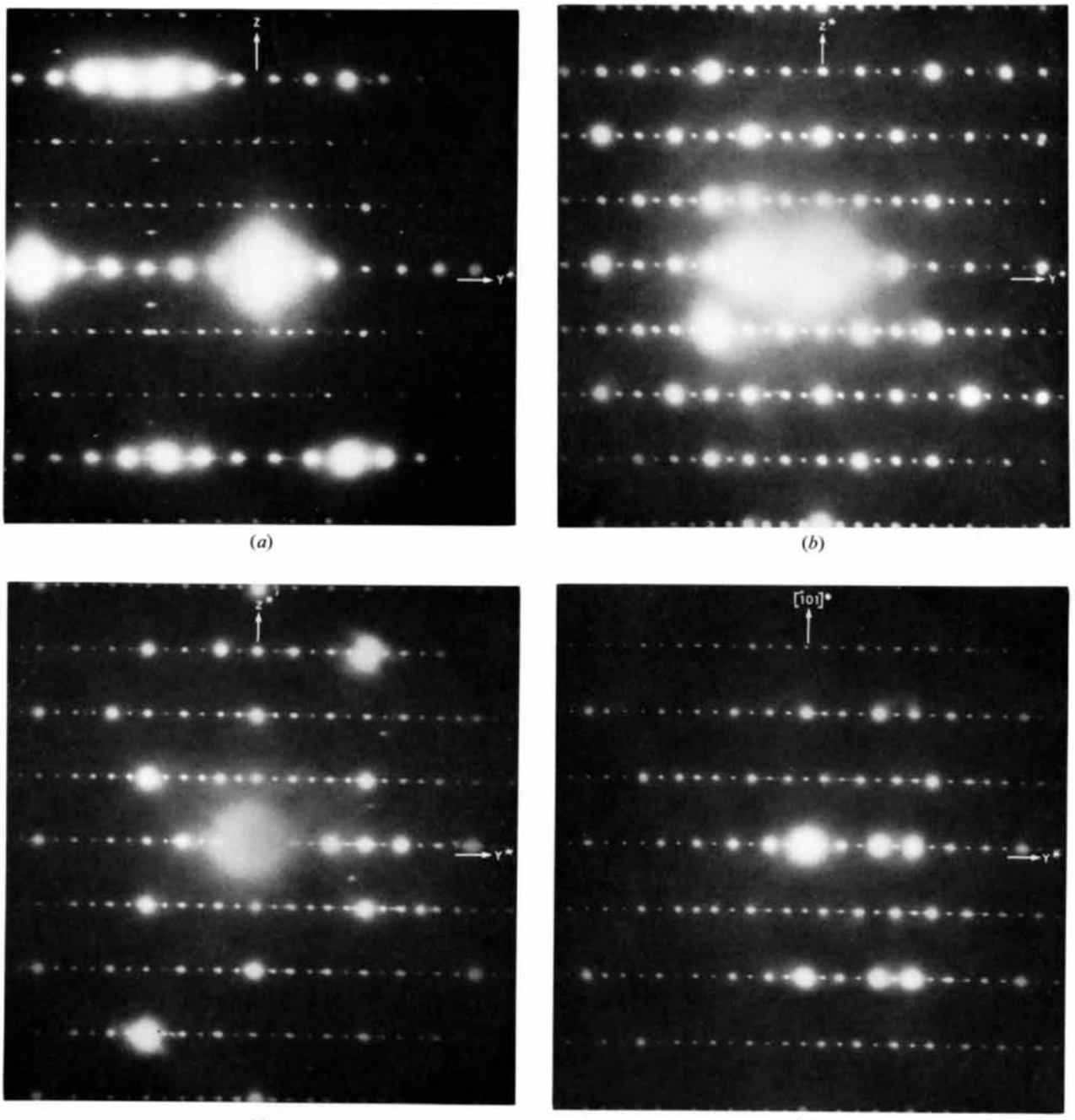

(*a*) (*b*) (*c*) (*d*)

Fig. 6. Electron diffraction patterns of amosite: (*a*) beam perpendicular to (100), giving strong reflexions of type $\bar{h},k,3h$; (*b*) specimen tilted by $11\frac{1}{2}°$ about the *y* axis to give the beam parallel to the *x* axis of one member of the twin, and strong reflexions of type $0kl$ (k even) together with weaker forbidden reflexions; (*c*) specimen tilted $11\frac{1}{2}°$ from (*a*) in the opposite direction from (*b*), giving strong reflexions of type $0kl$ (k even) from the other member; (*d*) specimen tilted a further 9° from (*c*) to give strong reflexions of type $\bar{h}kh$ (and therefore with k even and odd on alternate layer lines). All four photographs contain weak 'forbidden' reflexions.

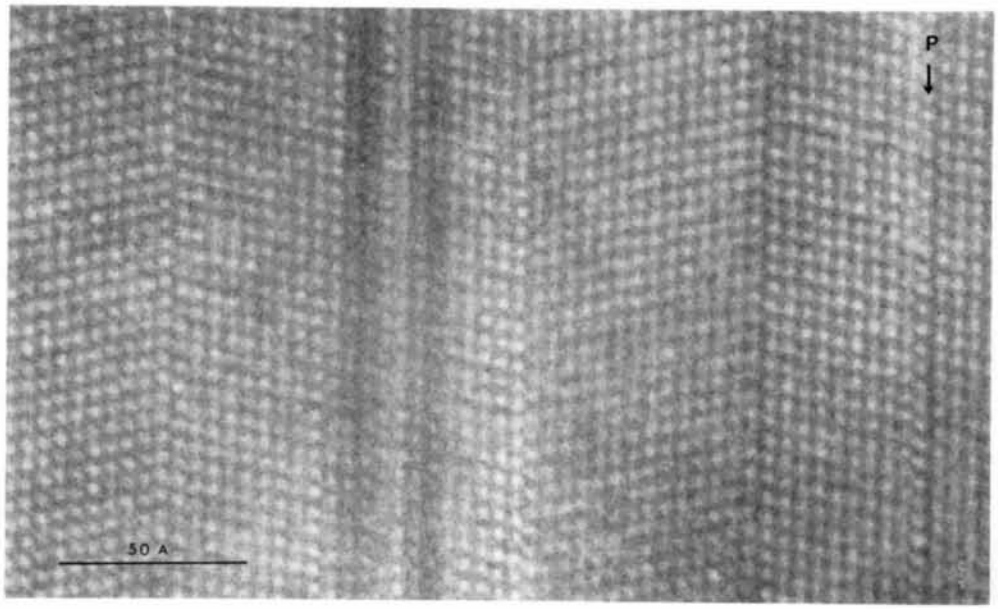

Fig. 7. High-resolution electron micrograph of amosite in the same orientation as the diffraction patterns of Fig. 2(*a*). The position of layers in the proto-amphibole configuration is marked *P*.

Fig. 9. Electron micrograph of crocidolite showing twin domains by diffraction contrast.

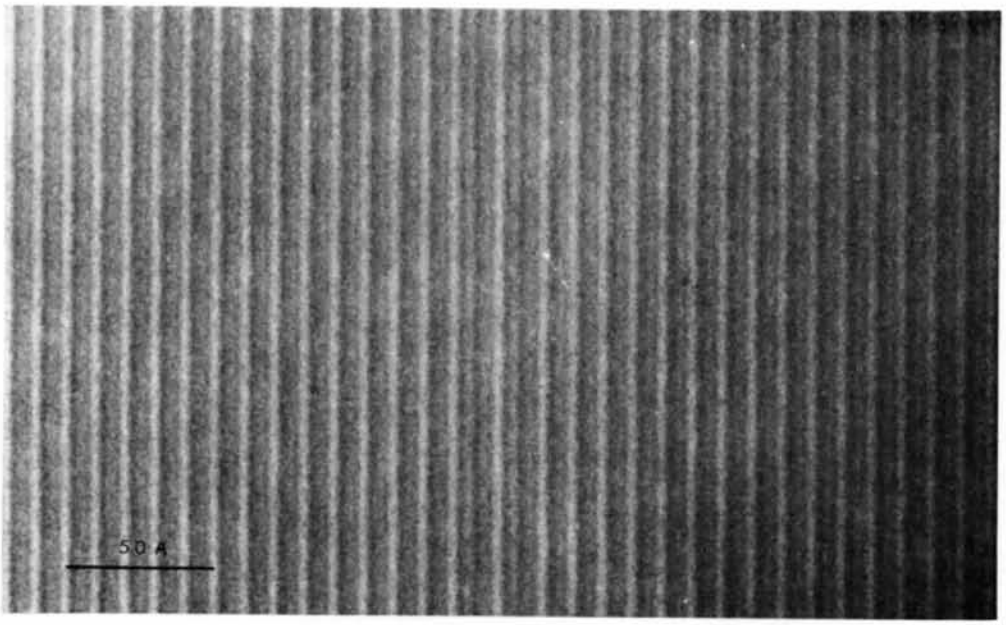

(*a*)

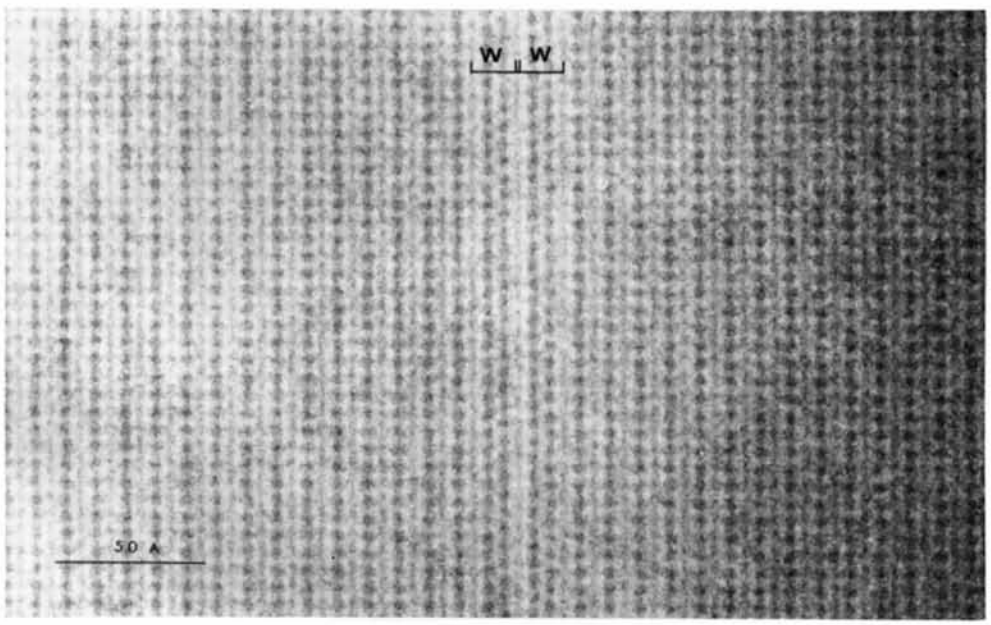

(*b*)

Fig. 10. Electron micrographs of amosite: (*a*) with the beam parallel to **x*** corresponding to Fig. 6(*a*); (*b*) with the beam parallel to the *x* axis of one set of twin lamellae corresponding to Fig. 6(*b*). Triple-chain lamellae are marked with *W*.

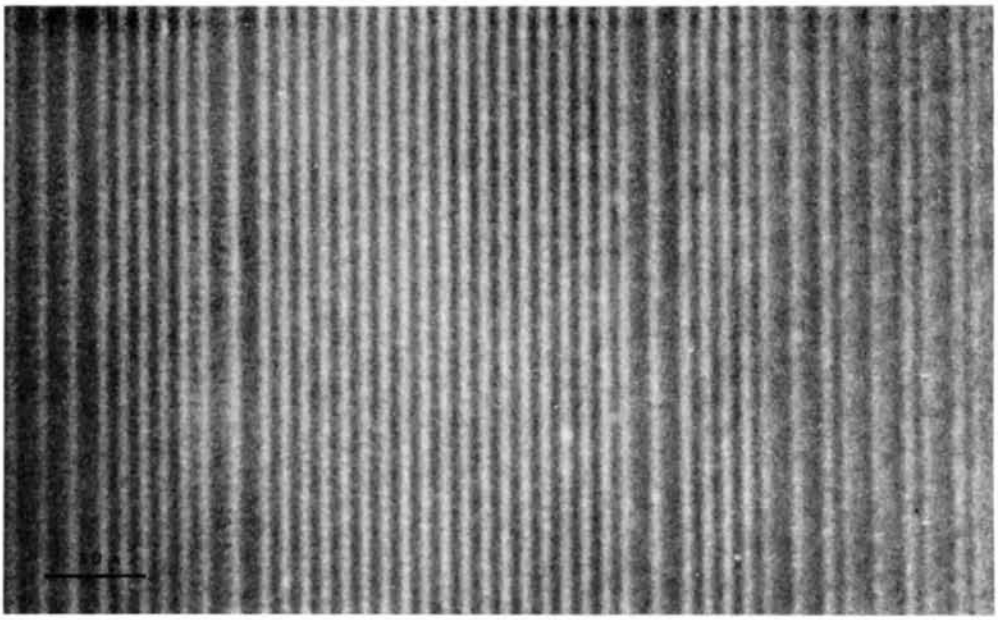

(*a*)

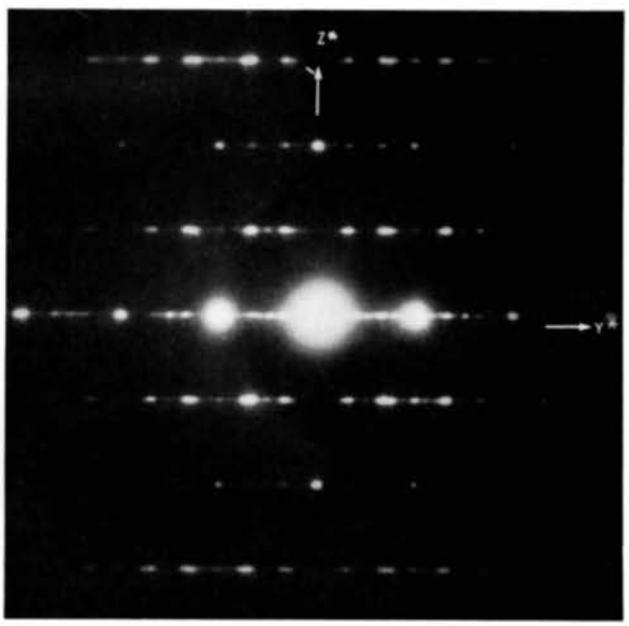

(*b*)

Fig. 11. (*a*) Electron micrograph of anthophyllite with the beam parallel to **x**, containing many Wadsley defects, probably corresponding to triple chains; (*b*) the corresponding diffraction pattern, with additional reflexions from the triple-chains domains.

[*To face p.* 797

Thus careful observation of the effects of tilting the crystal about y* shows that the pattern is not invariant as stated by Chisholm, but because of the doubled number of rational planes through a composite reciprocal lattice, together with compensatory changes on each side of the origin, the presence of some extension of reciprocal-lattice points parallel to x*, and the occurrence of inter-lamellar double reflexion, the development of off-centre Laue zones is far from obvious. However, the existence of the variation with orientation is evident from Fig. 6.

The streaking parallel to y* observed by Chisholm (1973) can be seen on the zero and third layer lines of Fig. 6(*a*), and rather less clearly on some of the other photographs.

4. High-resolution electron microscopy

A full interpretation of the details of the diffuse streaks parallel to x* and y* in the electron diffraction patterns of amosite has been achieved by means of high-resolution microscopy.

Fig. 7 shows the (200) and (001) lattice fringes of the same twinned crystal of amosite which provided the diffraction pattern of Fig. 2(*a*). The twinned lattice shows up clearly and it can be seen that the average thickness of the twin lamellae in this portion of this particular fibril is $10d_{200}(\sim 47$ Å). The off-set between adjacent lamellae appears to be $\pm c/2$ rather than $nc/3$ as postulated by Chisholm (1973). The average number of (200) fringes per lamella (from Fig. 7 and a number of similar pictures) is 15, and the frequency distribution is shown in Fig. 8. The number of lamellae counted is too small for the details of this distribution to be very significant, but it is not incompatible with a constant probability of 0·05 of twinning at each (200) plane.

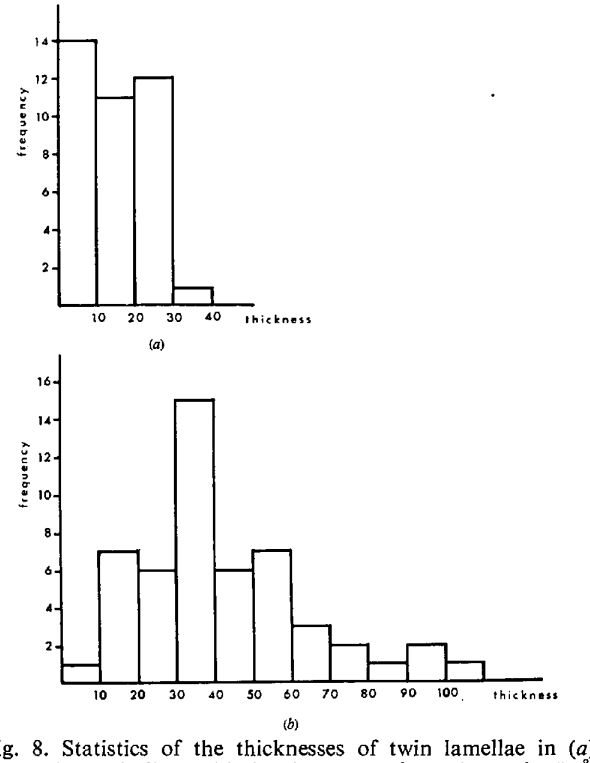

Fig. 8. Statistics of the thicknesses of twin lamellae in (*a*) amosite and (*b*) crocidolite, in terms of numbers of 4·7 Å lamellae.

Similar evidence has been obtained for twinning in crocidolite, but the frequency of the twin boundaries is much lower, and follows a very different distribution, also shown in Fig. 8. Fig. 9 shows a crocidolite specimen at lower magnification where the twinning is shown by diffraction contrast. Although the lamellae with the structure in one of the twin orientations again have a distribution of thicknesses, those in the other orientation are all of the same thickness or nearly so. This is clearly incompatible with the assumption of a constant probability of twinning on each (200) plane; and suggests a different structural control over the twinning.

A micrograph of amosite obtained with the beam parallel to the x* direction as in Fig. 6(*a*) is shown in Fig. 10(*a*). Lattice fringes with a spacing of ~ 9 Å ($b/2$), and some ill-defined intensity fluctuations between them fill most of the field, but in two places the main fringe spacing is increased to 13·5 Å. This is strongly suggestive of the presence of Wadsley defects of one or other of the types postulated by Chisholm (1973). With the beam parallel to the x axis of one component of the twin the result shown in Fig. 10(*b*) was obtained, with some two-dimensional resolution of structure both within the normal amphibole structure and in the regions of the Wadsley defects. The interpretation of these details, and a decision as to whether the intercalated layers consist of pyroxene chains or triple chains is not straightforward however, and is discussed in §6.

On the photographs that we have obtained of amosite we have counted four Wadsley defects in a total of about 1000 amphibole layers. In tremolite the corresponding numbers have been one in about 400.

Anthophyllite fibres have proved much more difficult to investigate than the clino-amphiboles, as they decompose much more readily in the electron beam. We have obtained electron micrographs only with the beam parallel to the x axis, and have only obtained one-dimensional fringe patterns probably because of the incipient decomposition. An example is shown in Fig. 11(*a*) and the corresponding diffraction pattern in Fig. 11(*b*). 13·5 Å fringes occur in appreciable numbers and tend to segregate into adjacent pairs and into more extensive domains. This leads to the appearance of discrete spots on the diffraction pattern related to the 13·5 Å repeat.

5. Structural interpretation of the twinning disorder

Fig. 12 shows projections down the y axis of the structures of grunerite, and anthophyllite (Finger, 1969,

1970). In grunerite the structure is divided up into identical lamellae, $\frac{1}{2}a \sin \beta$ thick, by the (200) planes on which the metal ions lie. In anthophyllite the (400) planes containing the metal ions also divide the structure into lamellae of the same thickness ($a/4$ for anthophyllite because of the doubled a axis) but the structures of the lamellae alternate markedly, half of them being similar to those in grunerite and the other half being quite different.

The term I-beam, introduced by Papike & Ross (1970) is a convenient nomenclature for discussion of the amphibole structure. Each I-beam consists of two silicate double chains sandwiching a strip of cations between them. In the projections in Fig. 12 the structure between a pair of (200) planes [(400) planes in anthophyllite] contains the superimposed contents of two silicate double chains belonging to two I-beams whose metal ions lie on successive (200) planes. In grunerite the two I-beams are in the same orientation. In anthophyllite the I-beams in both layers alternate in their orientation relative to [001], with the result that the lamellae lying between successive (400) planes alternate in nature: the first contains a superposition of silicate chains from two similarly disposed I-beams and the next contains a superposition of those from two oppositely disposed I-beams.

It was pointed out by Ito & Morimoto (1950) that anthophyllite could be regarded to a first approximation as corresponding to a clino-amphibole with twinning on every (100) plane of the clino structure. It is now known that the structure of anthophyllite (Finger, 1970) and the other orthoamphiboles (Papike & Ross, 1970; Irusteta & Whittaker, 1975) are more complicated in that the two silicate double chains of each I-beam are dissimilar in detail and are now traditionally described as the A and B chains. It is pairs of B chains belonging to like-oriented I-beams, and pairs of A-chains belonging to unlike oriented I-beams, that overlap in the [010] projection. However, for our present purpose the distinction between the A and B chains can be neglected.

As may be seen in Fig. 12, the 4·7 Å lamellae of anthophyllite that resemble clino-amphibole, are:

(i) twinned with respect to one another by reflexion and

(ii) translated by $c/2$ with respect to one another.

They are in fact related by a n-glide plane of the space group at the mid-plane of the intervening non-clino-like lamellae. It is to be expected that the relationship on the twin plane of grunerite will be identical with that in anthophyllite, and we therefore have strong grounds for accepting as real the indication in the micrograph of Fig. 7 that there is a translation of $c/2$ across the twinning plane, contrary to Chisholm's (1973) conclusion that translations of $nc/3$ occur in the twinned structure.

Chisholm's conclusion does not seem to have been based on diffraction evidence, but rather on the structural supposition that the translation would be controlled by displacement of a silicate chain relative to the metal ions within its own I-beam. It therefore ignored the stacking control exerted by the interlocking of the edges of adjacent I-beams.

In Fig. 12 the most electron-dense regions are those where there is a superposition of $2M1+2M4$. With the resolution available in the electron micrographs no other sites will be resolved and we should therefore see electron-dense islands outlining a cell $\frac{1}{2}a \times c$. One must conclude that Fig. 7 shows reversed contrast with the light spots representing the locations of $2M1+2M4$.

It is to be noted that there are places in Fig. 7 (indicated by P) where a translation by $c/2$ occurs on two successive (200) planes, so that there are almost adjacent regions which are not related by reflexion, but which are merely separated by two 4·7 Å lamellae like those which normally occur at the boundaries between twinned regions. This phenomenon can clearly be related to the structure of protoamphibole (Gibbs, 1969). In this structure all the I-beams centred at $y=0$ are in the same orientation, and all those at $y=0{\cdot}5$ are

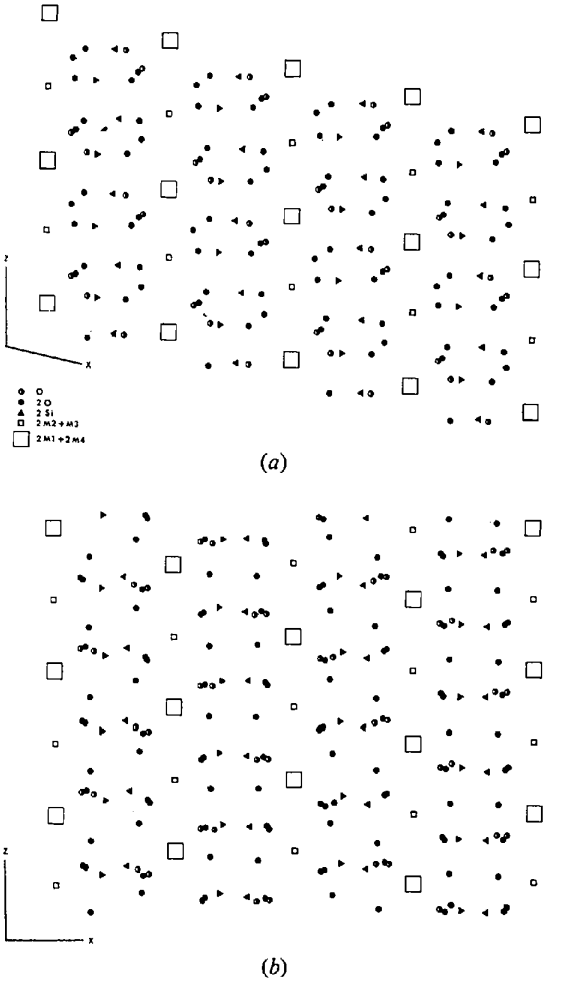

Fig. 12. Projections down the y axis of (*a*) grunerite and (*b*) anthophyllite.

in the opposite orientation. Thus every 4·7 Å lamella in the projection down y contains a superposition of silicate chains from oppositely disposed I-beams, and is shifted by $c/2$ with respect to its neighbours. The structure may be formally described as that of the clino-amphibole twinned on every (200) plane, instead of on every (100) plane as in anthophyllite. The observation of such situations in amosite is clearly to be expected if our structural interpretation is correct, since a finite probability of twinning on every (200) plane will lead to occasional twinning on successive (200) planes. A twin clino-lamella just 4·7 Å thick can therefore be considered to exist at each such boundary, although no (001) fringe of clino-form can in fact be defined. The frequency of such single-thickness twin lamellae has been included in Fig. 8. It may be noted that although two adjacent regions of amosite separated by a double fault of this kind have their axes in parallel orientation they are not coherent with one another. They are separated by a vector $a \sin \beta$ ($\mathbf{a}^*/a^*$), instead of **a** as they would be if they were coherent.

It was noted in §1 that X-ray evidence has long been known (Whittaker, 1950) for disorder in anthophyllite. This cannot be attributed to twinning on (100) in an orthorhombic structure, but the above discussion shows that it would easily occur as a result of stacking faults of exactly the same kind as those at the twin boundaries of grunerite. Such stacking faults would lead either to occasional small sequences of two or more successive 4·7 Å lamellae in the same orientation (a small clino-amphibole domain within the ortho-amphibole structure), or equally to sequences of 4·7 Å lamellae containing superpositions of oppositely oriented I-beams (a small proto-amphibole domain).

It was shown by Whittaker (1960) by crystal chemical arguments that the existence of ortho-amphibole is limited to compositions having small ions (originally thought to comprise only Mg and Li, but now known also to include Fe) at $M4$. The same criterion will inhibit a high probability of twinning except in the same circumstances. It is therefore to be expected that such stacking disorder arising during crystal growth should be limited to the ortho-amphiboles and to cummingtonite, grunerite and clinoholmquistite. This expectation is in line with the fact that the stacking faults observed in crocidolite have a lower probability and quite different statistics. They may well arise in a different way, such as by deformation.

6. The structural interpretation of the Wadsley defects

The structural nature of the two alternative kinds of Wadsley defects that may be expected to occur in amphiboles has been fully described by Chisholm (1973). In order to interpret the electron micrographs shown in Fig. 10 one needs to consider the projection of the grunerite structure down the [100] axis, together with corresponding projections of clinoferrosilite and a hypothetical triple-chain silicate of similar composition. Intercalated lamellae of these types are shown in Fig. 13.

A structural interpretation of Fig. 10(*a*) alone would be difficult because it is not clear how it is related to the symmetry elements in the structure. Comparison of Fig. 10(*b*) with Fig. 13, however, enables one to see that the mirror planes must lie along the rows of dark spots. These are of two kinds, one of which is darker than the other; one of these will correspond to the strips of structure containing $M3+4O$ and the other to the strips containing $2M4+4O$. The strips lying between these contain $M1+M2+4Si+8O$ and therefore have the highest density. As they appear light in the micrographs we therefore conclude that we have reversed contrast, and that the darkest spots will therefore lie on the $M3$ rows. In confirmation of these conclusions it may be pointed out that in the densely populated strips ($M1+M2+4Si+8O$) the atoms are distributed rather uniformly and could not be expected to show any appreciable resolution parallel to **z**. Our conclusion on contrast reversal is therefore supported by this consideration as well as by the apparent symmetry of the distribution of intensity in the **y** direction.

The above interpretation of the image in Fig. 10(*b*). leads to the conclusion that the Wadsley defects in amosite correspond to the intercalation of a layer of triple-chain structure, since the regions marked W contain a duplication of strips of $M3+4O$ with a separation of 4·5 Å similar to that shown in Fig. 13(*b*). After each such intercalation the following domain of amphibole structure can be seen to be displaced by $c/2$, as would be expected from the structure shown in Fig. 12(*b*). However, this would be equally true for a pyroxene intercalation and does not in itself provide evidence for our assignment.

Fig. 11(*a*) shows less resolution than Fig. 10, perhaps because of the incipient decomposition of the anthophyllite. However, there is a clear development of 13·5 Å fringes, of which the most natural interpretation is in terms of triple-chain structure. It would be conceivable that these fringes contained unresolved pairs of amphibole+pyroxene layers, but the segregated domains of these fringes would then require the unlikely development of a regular alternating sequence of amphibole and pyroxene layers. The existence of these segregations therefore provides additional indirect evidence in favour of our assignment.

7. Conclusions

Only a minority of the fibres visible in the electron microscope are suitable, in thickness, orientation, and isolation from other material, for investigation in the way we have described. The frequencies with which we have observed twinning defects and Wadsley defects in the various specimens may well, therefore, be unrepresentative. A method for obtaining information about these frequencies from X-ray fibre photographs will be presented in a subsequent paper.

We thank Professor J. S. Anderson for the use of the electron microscope. One of us (J.L.H.) acknowledges support from the Science Research Council. Parts of this work are included in a thesis to be presented by one of us (M.C.I.) to the University of Barcelona.

References

BUSECK, P. R. & IIJIMA, S. (1974). *Amer. Min.* **59**, 1–21.
CHISHOLM, J. E. (1973). *J. Mater. Sci.* **8**, 475–483.
CLARK, R. L. & RUUD, C. O. (1974). *Micron*, **5**, 83–88.
FINGER, L. W. (1969). *Min. Soc. Amer. Spec. Paper*, **2**, 95–100.
FINGER, L. W. (1970). *Carnegie Inst. Year Book*, **68**, 283–288.
GARROD, R. I. & RANN, C. S. (1952). *Acta Cryst.* **5**, 285.
GIBBS, G. V. (1969). *Min. Soc. Amer. Spec. Paper*, **2**, 101–109.
IRUSTETA, M. C. & WHITTAKER, E. J. W. (1975). *Acta Cryst.* B**28**, 145–150.

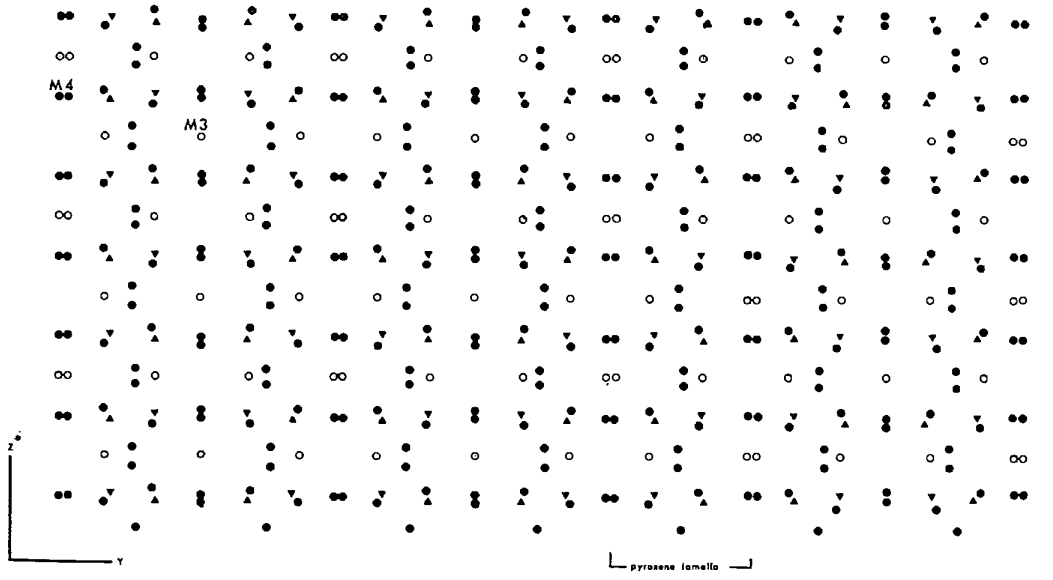

(*a*)

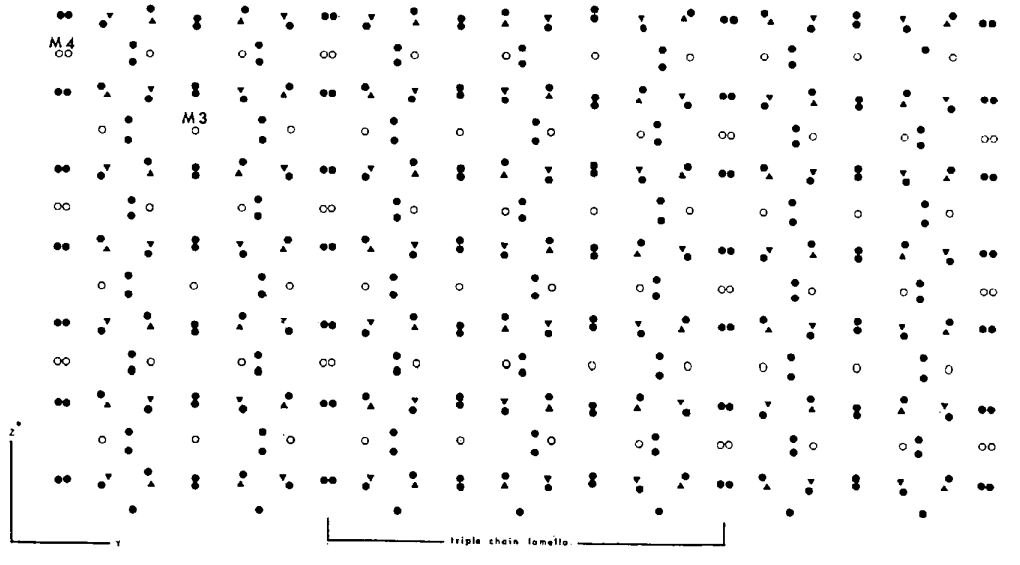

(*b*)

Fig. 13. Projections down the *x* axis of grunerite containing (*a*) an intercalated layer of pyroxene and (*b*) an intercalated layer of triple-chain structure. Metal ions – open circles, oxygen – filled circles, silicon – triangles.

ITO, T. & MORIMOTO, N. (1950). *X-ray Studies On Polymorphism*, pp. 42–49. Tokyo: Maruzen.
PAPIKE, J. J. & ROSS, M. (1970). *Amer. Min.* **55**, 1945–1972.
PINSKER, Z. G. (1953). *Electron Diffraction*, Translated by J. A. SPINK & E. FEIGL, p. 80. London: Butterworths.
RABBITT, J. C. (1948). *Amer. Min.* **33**, 263–323.
WARREN, B. E. (1930). *Z. Kristallogr.* **72**, 42–57.
WHITTAKER, E. J. W. (1949). *Acta Cryst.* **2**, 312–317.
WHITTAKER, E. J. W. (1950). *Brit. J. Appl. Phys.* **1**, 162.
WHITTAKER, E. J. W. (1960). *Acta Cryst.* **13**, 291–298.
WHITTAKER, E. J. W. & ZUSSMAN, J. (1961). *Acta Cryst.* **14**, 54–55.
ZVYAGIN, B. B. & GORSHKOV, A. I. (1969). *Methods for Electron Microscopy of Minerals*, Edited by G. S. GRITZAYENKO, B. B. ZVYAGIN, R. V. BOYARSKAYA, A. I. GORSHKOV, N. D. SAMOTOIN and K. E. FROLOVA, Chap. 6 (in Russian). Moscow: Nauka.

Acta Cryst. (1975). A**31**, 801

The Influence of Piezoelectric Coupling on Material Constants Determining Brillouin Scattering

BY G. MACHELEIDT

Sektion Mathematik/Physik, Pädagogische Hochschule Erfurt, DDR – 50 Erfurt, Nordhäuser Strasse 63, Germany (DDR)

(*Received* 19 *November* 1974; *accepted* 11 *February* 1975)

The piezoelectric modifications of the tensors of elastic, optical and photoelastic constants and their consequences on spontaneous and stimulated Brillouin scattering are discussed.

1. Basic equations

Starting with the expansion of the thermodynamic potential $f(U_{lm}, E_l)$ of a lossless medium with respect to the strain U_{lm} and the electric field E_l,

$$f(U_{lm},E_l)=f_o-\alpha_i E_i-\tfrac{1}{2}\alpha_{ik}E_iE_k -\tfrac{1}{3}\alpha_{ikl}E_iE_kE_l-\ldots+\tfrac{1}{2}\beta_{iklm}U_{ik}U_{lm} +\gamma_{ilm}E_iU_{lm}+\tfrac{1}{2}\gamma_{iklm}E_iE_kU_{lm}\,, \quad (1)$$

we obtain the equations of state we need for the macroscopic description of the Brillouin scattering process

$$P_i=-\frac{\partial f}{\partial E_i}=\alpha_i+\alpha_{ik}E_k+\alpha_{ikl}E_kE_l -\gamma_{ilm}U_{lm}-\gamma_{iklm}E_kU_{lm} \quad (2)$$

$$S_{ik}=\frac{\partial f}{\partial U_{ik}}=\beta_{iklm}U_{lm}+\gamma_{sik}E_s+\tfrac{1}{2}\gamma_{imik}E_lE_m\,. \quad (3)$$

Since we are dealing with high-frequency processes, namely ultrasonic and optical waves, in (2) and (3) the partial derivatives should be taken at constant entropy. That is the coefficients in (2) and (3) represent adiabatic constants. The optical constants α_{ik} and $\varepsilon_{ik}=\alpha_{ik}+\varepsilon_0\delta_{ik}$, the elastic constants β_{iklm}, the piezoelectric constants γ_{ikl}, the electrooptical constants α_{ikl} and the photoelastic constants γ_{iklm} give the connexions between the electric field E_i, the strain U_{lm} and the electric polarization P_i as well as the stress S_{ik}.

The linear piezoelectric coupling of the elastic and electric fields is given by the tensor of the piezoelectric constants γ_{sik}. Because of its index symmetry $\gamma_{sik}=\gamma_{ski}$ there are only 18 linearly independent components. This number is further reduced by the symmetry of the crystallographic class. For instance C_{6v} (6*mm*) (*e.g.* ZnO, CdS, ZnS, CdSe, CdTe, ZnTe) has three independent piezoelectric constants, C_{3v} (3*m*) (*e.g.* $LiNbO_3$) four constants, T_d ($\bar{4}3m$) (*e.g.* ZnS, GaAs, InSb, GaP, InAs, ZnSe) only one independent component. For media with inversion symmetry piezoelectricity does not exist.

We have to substitute the equations of state (2,3) into the field equations of Maxwell's and Newton's continuum theory

$$\left(\frac{\partial^2}{\partial x_i\partial x_k}-\frac{\partial^2}{\partial x_l\partial x_l}\delta_{ik}+\frac{\partial^2}{c_0^2\partial t^2}\delta_{ik}\right)E_k=-\mu_0\frac{\partial^2}{\partial t^2}P_i \quad (4)$$

$$\varrho\frac{\partial^2}{\partial t^2}U_i=\frac{\partial}{\partial x_k}S_{ik}\,. \quad (5)$$

2. Mixed acoustoelectromagnetic waves

At first we will consider only the linear terms and assuming plane waves with wave vectors $\mathbf{k}=k\mathbf{n}, \mathbf{K}=K\mathbf{N}$ and unit vectors $\mathbf{n},\mathbf{N}$ of the wave normals

$$E_l=\hat{E}_l\exp\left[i(\mathbf{kx}-\omega t)\right] \quad (6)$$

$$U_l=\hat{U}_l\exp\left[i(\mathbf{Kx}-\Omega t)\right], \quad (7)$$

we get the equations ($\mathbf{k}=\mathbf{K}, \omega=\Omega$):

$$(k_lk_k-k^2\delta_{ik}+\frac{\omega^2}{c_0^2}\varepsilon_{ik}^{\mathrm{rel}})E_k-i\mu_0\omega^2\gamma_{ikl}U_kk_l=0 \quad (8)$$

$$(\varrho\Omega^2\delta_{il}-\beta_{iklm}k_mk_k)U_l+i\gamma_{sik}E_sk_k=0\,. \quad (9)$$